# Current Saturation and Electrical Breakdown in Multiwalled Carbon Nanotubes

Philip G. Collins, M. Hersam, M. Arnold, R. Martel, and Ph. Avouris*
*IBM T. J. Watson Research Center, Yorktown Heights, New York 10598*
(Received 28 August 2000)

We investigate the limits of high energy transport in multiwalled carbon nanotubes (MWNTs). In contrast to metal wires, MWNTs do not fail in the continuous, accelerating manner typical of electromigration. Instead, they fail via a series of sharp, equally sized current steps. We assign these steps to the sequential destruction of individual nanotube shells, consistent with the MWNT's concentric-shell geometry. Furthermore, the initiation of this failure is very sensitive to air exposure. In air failure is initiated by oxidation at a particular power, whereas in vacuum MWNTs can withstand much higher power densities and reach their full current carrying capacities.

DOI: 10.1103/PhysRevLett.86.3128 PACS numbers: 73.50.Fq, 72.10.Di, 73.61.Wp

Electromigration, rather than fabrication, is a fundamental problem limiting the further miniaturization of metallic wires. Electromigration is a nonthermal, current-assisted diffusion process initiated at points of current flux divergence such as grain boundaries [1], and it strictly limits the current carrying capacity of a wire. This current limit is approximately 10 $nA/nm^2$ in noble metals, a severe restriction for nanometer-sized wires. Carbon nanotubes, with their strong carbon-carbon bonds, are much less sensitive to electromigration and have current carrying capacities exceeding 10 $\mu A/nm^2$ [2,3]. Thus metallic nanotubes, particularly multiwalled carbon nanotubes (MWNTs), are promising as reliable, nanometer-sized metallic wires and microcircuit interconnects. Although electrical transport in carbon nanotubes is a subject of intense study, most of the experimental and theoretical work until now has focused on the low energy regime [3,4]. Very little consideration has been given to the high field, room temperature characteristics which make these nanometer conductors technologically relevant.

In this Letter, we present results on the high bias transport in MWNTs with special emphasis on the mechanism and the factors that control electrical breakdown in these materials. In contrast to metal wires, MWNTs do not fail via electromigration. Instead, we find that they fail in a series of sharp steps associated with the destruction of individual nanotube shells. Unlike the case of conductance quantization, these steps are regularly spaced in current regardless of the applied voltages. This spacing is due to high bias current saturation in MWNTs, similar to that reported for single-walled nanotubes (SWNTs) [5].

MWNT test structures are produced by depositing arc-grown MWNTs dispersed in dichloroethane onto $SiO_2$ substrates prepatterned with Au/Ti electrodes (250 nm wide, 40 nm high). We choose devices in which single MWNTs make electrical contact to six unequally spaced electrodes, so that independent four-probe measurements can be obtained from different segments of the same MWNT. In addition, contact resistances can be estimated both before and after the electrical failure of a particular segment. The low contact resistances of our samples (typically below 1 k$\Omega$) allow an appreciable voltage to be dropped across the nanotube, which is critical for achieving breakdown in the nanotube body as opposed to at the metal contact. Finally, the multiprobe configuration allows breakdown events on different segments of the same nanotube to be directly compared, ensuring that the measurements reflect intrinsic properties of a particular sample. The breakdown experiments are performed by applying a constant stress voltage to the MWNT while simultaneously acquiring an uninterrupted record of the total current and the voltage drops across each nanotube segment.

Figure 1 shows the time-resolved electrical breakdown of an 8 nm diameter MWNT in air. Upon raising the (four-probe) stress to 1.7 V, the current becomes a function of time $I(t)$, a portion of which is shown in Fig. 1a. After first decreasing slowly, $I(t)$ drops in a series of seven abrupt steps before stabilizing. The plot shows a remarkably regular staircase with step sizes of about 12 $\mu$A.

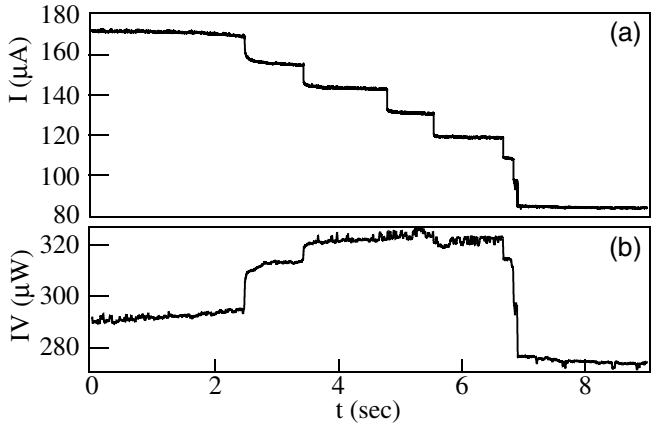


FIG. 1. Time trace of the current $I(t)$ and dissipated power $P(t)$ during a MWNT breakdown. (a) The current exhibits a staircase of stable currents separated by 12 $\mu$A steps. (b) $P(t)$ indicates that stable values of current (or MWNT resistance) occur only when the power is below 300 $\mu$W (note that the four-probe voltage across the segment is not constant as the segment fails).

 0031-9007/01/86(14)/3128(4)$15.00 

Similar plots of the conductance ($G = I/V$) and dissipated power ($P = IV$) for the same segment are not evenly spaced, since in a four-probe configuration the voltage across the failing segment increases from step to step. Nevertheless, the time dependence of $P$ (Fig. 1b) does contain important additional information. The initial, slowly increasing resistance leads to a gradual increase in $P$. The first abrupt failure occurs when $P$ reaches a value of about 300 $\mu$W, and only after the seventh step does $P$ again fall below 300 $\mu$W. At this time, the MWNT resistance also stabilizes, and remains stable unless a larger bias is applied. This observation suggests that a power threshold $P_{\text{thresh}}$ must be exceeded for the initiation of the stepwise breakdown. A comparison among many different MWNTs indicates $P_{\text{thresh}}$ to be roughly constant for the initiation of breakdown in air, with values falling in a range of 280 to 350 $\mu$W independent of MWNT diameter [6].

Oxygen in the ambient plays an important role in the stability of MWNTs and their breakdown dynamics. As a demonstration, Fig. 2 compares the breakdown behavior of two adjacent segments of a 14 nm diameter MWNT, one broken in vacuum and the other in air. First, the MWNT is stressed in high vacuum until failure of one segment (A). After checking the current-voltage characteristic ($I$-$V$) of segment B to show that it has been unaffected by the first stress (dashed line in Fig. 2) [7], the MWNT is exposed to air and stressed again until segment B fails. The breakdown of segment B (shown in the inset) is substantially the same as for Fig. 1, with initiation occurring at a power of 315 $\mu$W and a regular staircase in $I(t)$ with step sizes of both 12 and 24 $\mu$A.

Such experiments show that the primary effect of placing the sample in vacuum is to allow much higher powers to be reached before breakdown. In vacuum, segment B clearly withstands powers exceeding 400 $\mu$W with no ill effects, and the vacuum failure of segment A does not occur until 520 $\mu$W, at which point the $I$-$V$ is nearly horizontal, i.e., the current is nearly saturated. Once failure is initiated at this high power, it occurs approximately 1000 times more rapidly than in air [8]. This can be understood in terms of the theory of unimolecular decomposition reactions, according to which the decomposition rate increases strongly with excess energy above the threshold energy [9]. Of course, we cannot rule out that the presence of oxidants may also slow the breakdown by binding up defects (dangling bonds) in the nanotube.

Because MWNTs have higher power thresholds in vacuum, we can extend the $I$-$V$ measurements to the high current, extremely nonlinear regime shown in Fig. 2. Above the low bias, linear (or slightly superlinear [10]) regime, MWNT $I$-$V$s incorporate a point of inflection above which $dI/dV$ decreases towards a sample-dependent saturation current. Similar current saturation at high bias has been reported recently for SWNTs [5] and has been attributed to both electron-phonon scattering processes [5] and Bragg backscattering [11]. Although the exact saturation current of MWNTs is sample dependent, we have never observed

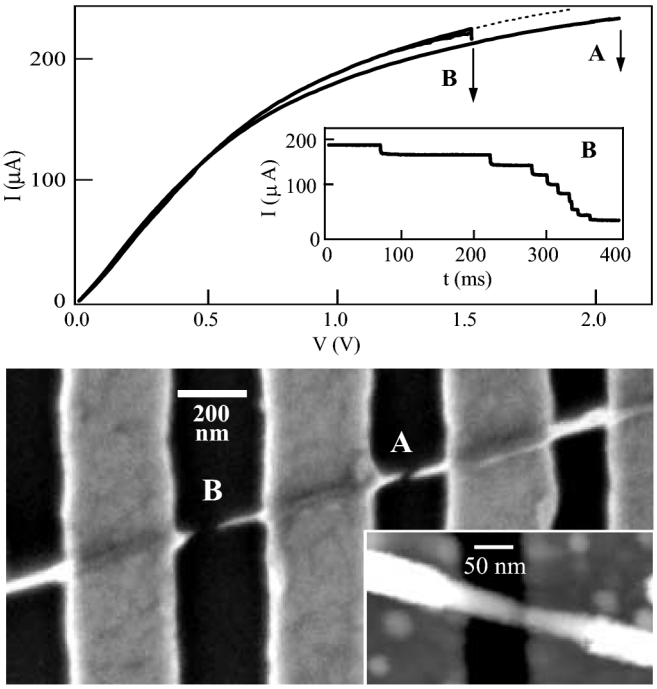


FIG. 2. (top) Four probe $I$-$V$s and $I(t)$ for two adjacent segments of a MWNT. Segment A is electrically broken in high vacuum, while segment B is broken in air. Before failure, both segments have nearly identical $I$-$V$ characteristics in vacuum, and both segments can withstand more than 400 $\mu$W of power (segment B in vacuum shown as dashed line). Vacuum breakdown occurs in segment A at 2.2 V and 235 $\mu$A, and at this high power proceeds to completion in less than 1 ms. In air, segment B exhibits a much slower breakdown initiated at a power of 320 $\mu$W (inset, the first step at $t = 0$ is not shown). (bottom) SEM imaging of the damaged segments shows significant thinning of the remaining MWNT material in both segments, with a wider gap and greater thinning for the segment broken in air. Pausing the stress midway through the breakdown produces a thinned but unbroken MWNT (inset).

breakdown below the point of inflection in the $I$-$V$, either in air or in vacuum. This observation suggests that the onset of saturation and the eventual breakdown process are linked to a common dissipative process, most likely involving the excitation of high energy optical or zone boundary phonons [5].

In addition to investigating MWNT breakdown electrically, we have imaged MWNTs at various stages of breakdown using atomic force microscopy (AFM) and scanning electron microscopy (SEM). Images of failed MWNTs show surprisingly large quantities of lost carbon, in stark contrast to the small gaps observed when metallic wires fail via electromigration [12]. As seen in Fig. 2 (bottom), the remaining MWNT material in the broken segments A and B both exhibit decreased diameters compared to the adjacent, unbroken segments. Because the breakdown occurs in discrete steps, we have also been able to stabilize MWNTs at various intermediate steps. Imaging these intermediate states shows similar diameter thinning, but without resolvable gaps, as shown in the inset. Contact

resistances in these intermediate states are usually found unchanged, in agreement with the postbreakdown SEM imaging.

The MWNT thinning indicates a loss of individual carbon shells, even far from the point of failure, and suggests that the steps in $I(t)$ are due to shell-by-shell failure of the MWNT. If so, then the number of steps should depend upon the MWNT diameter, which we show in Fig. 3a. *In situ* transmission electron microscopy experiments have resolved similar thinning and the shell-by-shell loss of material due to both oxidation [13] and repeated electrostatic shocks [14].

The larger amount of missing material and the excessive thinning in segment B are typical of MWNTs broken in air. Combined with the lower $P_{\text{thresh}}$ observed in air, this observation strongly suggests that oxidation can assist the breakdown [15]. Indeed, we have found that MWNT breakdown in inert gases proceeds as in vacuum, with high power thresholds and less loss of material. We note, however, that our electrical measurements primarily record the initiation of failure; much of the observed carbon loss occurs after this initiation, since defects and dangling bonds then provide various chemical pathways for oxidation to proceed.

Images such as Fig. 2 also indicate that MWNT breakdown usually occurs midway between two electrodes,

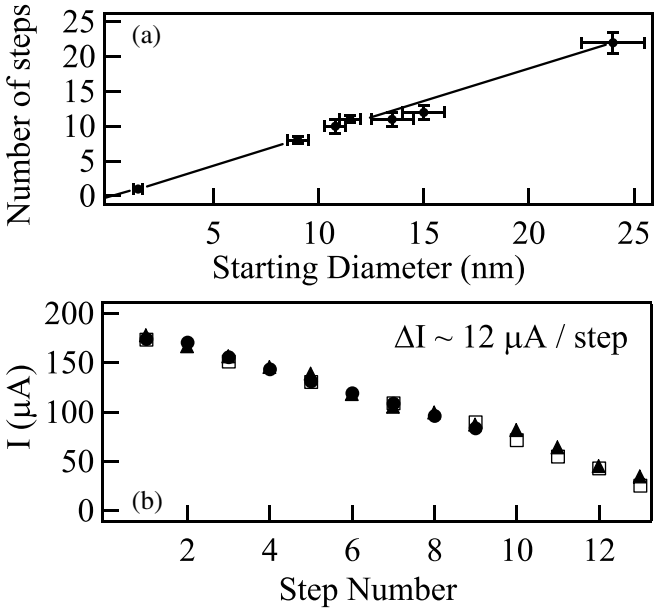


FIG. 3. (a) A comparison of multiple samples shows a proportionality between the number of steps in the breakdown $I(t)$ and the MWNT diameter, consistent with a shell-by-shell mechanism. (b) Further comparison of the current observed at each step of the breakdown reveals remarkable similarities. Here we plot the mean current at each step in $I(t)$ for three different MWNTs with varied segment lengths. The steps are sequentially numbered beginning with the plateau at $I = 170\ \mu$A, which is the highest current reached by all three samples. Not only do different samples lose current at the same average rate of 12 $\mu$A per step, but the current values themselves are nearly identical, independent of the MWNT segment length.

which is precisely where dissipative self-heating will produce a peak temperature $T_p$. Taking a power $P_{\text{thresh}} = 300\ \mu$W uniformly distributed along the MWNT, we can estimate $T_p$ based on a simple heat transfer analysis [16]. Unfortunately, just as for carbon fibers and graphite, the experimental values of MWNT thermal conductivity $K$ range widely, from $K = 25$ W/mK [17] to $K = 200$ W/mK [18]. A conservative estimate using the higher $K$ gives $T_p = 500$–$700\,^{\circ}$C, a range which agrees with the known temperatures for thermal oxidation of MWNTs [13] and for the oxidation of damaged graphite [19]. Therefore, the breakdown of MWNTs may be intimately connected with self-heating and the reaction of nanotube shells with oxygen. However, spontaneous oxidation is probably not the primary cause of electrical breakdown, since oxidation at such low temperatures cannot proceed without the prior formation of defects [13], and thermal vaporization in vacuum would require a $T_p$ exceeding 2800 °C. Instead, the initiation of both breakdown and oxidation probably depends upon local, nonequilibrium effects including defect creation due to the extreme current densities exceeding 1 $\mu$A/nm$^2$ (at 12 $\mu$A per shell) [15,20]. Sample-dependent properties such as curvature-induced strain and the concentration of preexisting defects may also contribute to this initiation and be factors in determining $P_{\text{thresh}}$ for MWNTs in vacuum.

The breakdown behaviors described above have been observed on many MWNT samples, at 300 and 77 K, both in air and in vacuum. Figure 3 summarizes data obtained in air at 300 K. Figure 3a shows the total number of discrete steps $N$ observed in the breakdown $I(t)$ as a function of the initial diameter of the MWNT determined by AFM. This figure identifies a dependence between $N$ and the MWNT diameter, which to first approximation is proportional to the number of shells in the MWNT. Figure 3a also includes a measurement of an individual SWNT. We find that unlike MWNTs, SWNTs fail in a single, featureless step. This fact, along with the apparent proportionality between $N$ and diameter, further supports assigning the observed steps in $I(t)$ to the failure of individual MWNT shells.

A most interesting effect is observed when the $I(t)$ breakdown of different samples is directly compared. As noted above, $I(t)$ rather than $G(t)$ forms the most regularly spaced staircase, and we find the spacing to be sample independent. Figure 3b shows the mean current value $I_i$ at each step in the $I(t)$ staircase for three MWNTs of different diameters and four-probe resistances. Not only do the three data sets have the same average slope of 12 $\mu$A per step, but the $I_i$ values themselves are in exceptional agreement. If allowance is made for "missing" plateaus in a particular $I(t)$ trace (perhaps due to experimental time resolution limits), the currents $I_i$ from various MWNTs exhibit remarkable agreement, independent of whether the MWNT failed in vacuum or in air.

The constant step size $\Delta I_i = 12\ \mu$A can be considered a direct effect of the loss of individual carbon shells if we take into account the current saturation observed in Fig. 2. We propose that in the high bias, current saturation limit, each shell of the MWNT is individually saturated in a manner similar to the single shell saturation of SWNTs [5]. During breakdown, the sequential removal of shells will produce evenly spaced steps $\Delta I_i$ as the current carrying capacity of each shell is lost. The constant slope in Fig. 3b indicates a current carrying capacity of 12 $\mu$A per shell, independent of the decreasing shell diameter as expected for an electron-phonon scattering mechanism.

In fact, every shell in a MWNT need not be saturated in order to observe this constant step size. Consider the different shells of a MWNT as independent, parallel conductors, each with a different coupling resistance to the outermost shell (which is in direct contact with the metal electrodes). In this geometry, outer shells contribute more to the total conductance than do inner shells because of their lower coupling resistance to the external electrodes. Similarly, outer shells will carry the greatest proportion of the total current and can saturate before the MWNT as a whole is saturated. At high voltages these shells may be unable to carry additional current, but current injection into the inner shells results in a nonzero $dI/dV$. Under these conditions, with an unknown distribution of saturated and unsaturated shells, the breakdown of the outermost shells will still result in fixed drops $\Delta I_i$ as we have observed.

Our observations indicate that many shells can contribute to the high bias conductance of a MWNT, in contrast to the single-shell model believed to hold in the low bias, low temperature regime [4]. This difference is probably due to the energy dependence of intershell coupling. At high biases, the effective coupling may improve due to both electron injection at the contacts and also enhanced electron-electron scattering, which will tend to relax momentum conservation requirements among shells. Improved models of MWNT conduction need to be developed in order to further understand our observations of current saturation and the uniform current steps during breakdown.

In summary, we have measured the high bias conduction limits of individual MWNTs. In air, conduction is limited by a power threshold, above which breakdown and oxidation of the MWNT is initiated. In vacuum, the threshold for failure is raised, but conduction remains limited by a sample-dependent current carrying capacity. When these thresholds are exceeded, a MWNT fails via a unique staircase breakdown as its carbon shells are individually destroyed.

We thank J. Tersoff and S. Roche for valuable discussions, and B. Ek for expert technical assistance. M. H. and M. A. acknowledge the support of IBM summer internships.

*Corresponding author.
Email address: avouris@us.ibm.com

[1] A. Christou, *Electromigration and Electronic Device Degradation* (Wiley-Interscience, New York, 1994).
[2] H. Dai, E. W. Wong, and C. M. Lieber, Science **272**, 523 (1996).
[3] S. Frank, P. Poncharal, Z. L. Wang, and W. A. deHeer, Science **280**, 1744 (1998).
[4] A. Bachtold, C. Strunk, J.-P. Salvetat, J.-M. Bonard, L. Forro, T. Nussbaumer, and C. Schenenberger, Nature (London) **397**, 673 (1999).
[5] Z. Yao, C. L. Kane, and C. Dekker, Phys. Rev. Lett. **84**, 2941 (2000).
[6] One might expect the threshold power to be length dependent, but we have not performed four-probe measurements on longer segments. MWNT segment lengths range from 100 to 300 nm in our experiments.
[7] For comparison with the four-probe values, the voltages for segment B in air have been corrected using the known contact resistance values.
[8] Generally our measurements are performed with sampling rates of 5 kHz. Observing the complete $I(t)$ staircase in vacuum requires sampling rates of at least 10 MHz, which we have performed on two-probe samples with electrode spacings up to 2500 nm.
[9] P. J. Robinson and K. A. Holbrook, *Unimolecular Reactions* (Wiley-Interscience, New York, 1972).
[10] Some MWNT segments exhibit superlinear $I$-$V$s with the form $I = aV + bV^{3/2}$. This nonlinear behavior suggests space-charge limited transport, and we attribute it to contact effects, particularly since adjacent segments exhibit this behavior to different extents. See, for example, M. A. Lampert and P. Mark, *Current Injection in Solids,* edited by H. G. Booker and N. DeClaris, Electrical Science (Academic Press, New York, 1970).
[11] M. P. Anantram, Phys. Rev. B **62**, 4837 (2000).
[12] H. Park, A. K. L. Lim, A. P. Alivisatos, J. Park, and P. L. McEuen, Appl. Phys. Lett. **75**, 301 (1999).
[13] P. M. Ajayan *et al.,* Nature (London) **362**, 522 (1993).
[14] J. Cumings, P. G. Collins, and A. Zettl, Nature (London) **406**, 586 (2000).
[15] T. Schmidt, R. Martel, R. L. Sandstrom, and Ph. Avouris, Appl. Phys. Lett. **73**, 2173 (1998).
[16] As a conservative estimate, we take the MWNT to be a solid cylinder and neglect the radial anisotropy in power dissipation or thermal conductivity $K$. For this case, the peak temperature at the midpoint of the MWNT segment is $T_p = P_{\text{thresh}} \times \text{Length}/(8K \times \text{Area}) + 293$. See, for example, M. Jakob, *Heat Transfer* (John Wiley & Sons, New York, 1949).
[17] W. Yi, L. Lu, Z. Dian-lin, Z. W. Pan, and S. S. Xie, Phys. Rev. B **59**, R9015 (1999).
[18] Philip Kim (private communication).
[19] S. M. Lee, Y. H. Lee, Y. G. Hwang, J. R. Hahn, and H. Kang, Phys. Rev. Lett. **82**, 217 (1999).
[20] In fact, the generation of defects may affect the thermal conductivity considerably. See, for example, J. Che, T. Cagin, and W. A. Goddard III, Nanotechnology **11**, 65 (2000).